Brain capillary transit time heterogeneity in healthy volunteers measured by dynamic contrast-enhanced T1-weighted perfusion MRI

Larsson, Henrik B.W.; Vestergaard, Mark B.; Lindberg, Ulrich; Iversen, Helle K.; Cramer, Stig P.

Published in:
Journal of Magnetic Resonance Imaging

DOI:
10.1002/jmri.25488

Publication date:
2017

Document version
Publisher's PDF, also known as Version of record

Brain Capillary Transit Time Heterogeneity in Healthy Volunteers Measured by Dynamic Contrast-Enhanced T_1-Weighted Perfusion MRI

Henrik B.W. Larsson, DMSc,[1,2]* Mark B. Vestergaard, MSc,[1] Ulrich Lindberg, PhD,[1] Helle K. Iversen, DMSc,[2,3] and Stig P. Cramer, PhD[1]

Purpose: Capillary transit time heterogeneity, measured as CTH, may set the upper limit for extraction of substances in brain tissue, e.g., oxygen. The purpose of this study was to investigate the feasibility of dynamic contrast-enhanced T_1 weighted MRI (DCE-MRI) at 3 Tesla (T), in estimating CTH based on a gamma-variate model of the capillary transit time distribution. In addition, we wanted to investigate if a subtle increase of the blood–brain barrier permeability can be incorporated into the model, still allowing estimation of CTH.

Materials and Methods: Twenty-three healthy subjects were scanned at 3.0T MRI system applying DCE-MRI and using a gamma-variate model to estimate CTH as well as cerebral blood flow (CBF), cerebral blood volume (CBV), and permeability of the blood–brain barrier, measured as the influx constant K_i. For proof of principle we also investigated three patients with recent thromboembolic events and a patient with a high grade brain tumor.

Results: In the healthy subjects, we found a narrow symmetric delta-like capillary transit time distribution in basal ganglia gray matter with median CTH of 0.93 s and interquartile range of 1.33 s. The corresponding residue impulse response function was compatible with the adiabatic tissue homogeneity model. In two patients with complete occlusion of the internal carotid artery and in the patient with a brain tumor CTH was increased with values up to 6 s in the affected brain tissue, with an exponential like residue impulse response function.

Conclusion: Our results open the possibility of characterizing brain perfusion by the capillary transit time distribution using DCE-MRI, theoretically a determinant of efficient blood to brain transport of important substances.

Level of Evidence: 2

J. MAGN. RESON. IMAGING 2017;45:1809–1820

Dynamic contrast-enhanced T_1-weighted MRI (DCE-MRI) enables measurement of the blood–brain barrier (BBB) permeability, i.e., the permeability surface area (PS) product, cerebral blood flow (CBF), and the cerebral blood volume (CBV).[1–3] The advantage of DCE-MRI compared with dynamic susceptibility contrast T_2^* weighted MRI, is a robust relationship between the MR signal and the contrast agent (CA) concentration, allowing conversion of tissue MR signal as well as arterial and venous MR signal to CA concentration by the relevant MR signal equation. In addition, if the BBB permeability is abnormally high, it is still possible to estimate both the CBV and the total distribution volume (V_d), which include the CA accessible extravascular interstitial space.[2,3] Also, DCE is able to provide quantitative measures of both perfusion and permeability parameters, while maintaining a high spatial resolution and low sensitivity to susceptibility artifacts.

The disadvantage of DCE-MRI is low tissue MR signal during bolus passage, related to the fact that the CA is

View this article online at wileyonlinelibrary.com. DOI: 10.1002/jmri.25488

Received May 5, 2016, Accepted for publication Sep 6, 2016.

*Address reprint requests to: H.B.W.L., Functional Imaging Unit, Department of Clinical Physiology, Nuclear Medicine and PET, Rigshospitalet, Glostrup, University of Copenhagen, Nordre Ringvej 57, 2600 Glostrup, Denmark. Email: henrik.larsson@regionh.dk

From the [1]Functional Imaging Unit, Department of Clinical Physiology, Nuclear Medicine and PET, Rigshospitalet, Glostrup, Denmark; [2]Institute of Clinical Medicine, The Faculty of Health and Medical Sciences, University of Copenhagen, Denmark; and [3]Department of Neurology, Rigshospitalet, Glostrup, Denmark

normally confined to the vascular space in situations with intact BBB resulting in a low contrast-to-noise ratio (CNR). In addition, full coverage of the brain is not compatible with the high temporal resolution of 1–2 s required to estimate perfusion from the bolus passage and, therefore, only four to eight slices can be obtained with such a high time resolution. Higher scanner field strengths and faster sequences, e.g., multiband sequences, optimized 3D sequences may ameliorate these problems. Furthermore, integration of DCE in clinical practice is currently limited, partly due to the complexity of the analysis methods, the lack of standardization in regards to acquisition and analysis protocols and the limited availability of reference values for the various pharmacokinetic (PK) parameters for normal and pathological brain tissues.

Capillary transit time heterogeneity (CTH) may be a determinant of delivery of substances from the blood to the brain tissue as originally suggested by Kuchinsky and Paulson.[4] A recent study showed how an abnormal increase in CTH theoretically could hamper an efficient oxygen extraction to the brain tissue.[5] Normally, neural activation gives rise to an increase in local brain tissue perfusion by recruitment of previously nonperfused capillaries.[4,6] The capillary perfusion thus becomes more homogeneous.[4,6] The hypothesis put forward is that if brain diseases affect the microvascular regularization, e.g., affecting the pericytes controlling the flow through the capillaries, a pathological inhomogeneous perfusion pattern ensues, which may become even more pronounced as perfusion increases. As a consequence and in contrast to the normal microvascular regulation, transit times through the capillaries vary more than normal, and the extraction of blood substances in high flow capillaries will decrease due to a reduction of the extraction fraction, a consequence of the Crone-Renkin equation,[7,8] and if severe enough the flux might also decrease.

Thus, a situation may arise where both high and low flow capillaries contribute to an overall reduction in flux of substances from blood to brain tissue. This scenario is evidently dependent on the PS product of the actual substance in focus. Therefore, CTH dependent blood to tissue flux is relevant for substances with a low to moderate value of the PS product, where transport over the BBB is diffusion limited. For substances with a high PS product, the flux from blood to tissue is flow (perfusion) limited, and the actual perfusion distribution pattern is of minor importance. If the oxygen transport from blood to tissue over the BBB is diffusion limited, a subject of considerable scientific interest,[9] then CTH may theoretically become a determinant of the maximal oxygen extraction fraction possible.[5] If diseases affect the normal regulation of local perfusion, an increase in perfusion may in fact aggravate a possible pre-existing hypoxic state and the tissue may become even more hypoxic.[5]

This idea could also have an important impact for oxygen delivery in brain tumors, where the normal capillary architecture is severely disturbed, and high perfusion and hypoxia may co-exist in some parts of the tumors. For this reason, methods allowing us to estimate the distribution of capillary transit times in healthy and diseased tissue may be of importance, and CTH estimation may provide new important physiological information like conventional measurements of other tissue parameters, such as CBF or CBV.

The purpose of this study is to develop a method that enables CTH as well as CBF measurements derived from DCE-MRI in normal white and deep gray matter. Furthermore, we wish to be able to account for a subtle increase of the BBB permeability, characterized as a unidirectional transport from blood to tissue without any back diffusion, which may be encountered in various brain pathologies such as white matter of multiple sclerosis patients, Alzheimer's disease, vascular cognitive impairment, stroke, and low grade brain tumors.[10–12]

Materials and Methods

Theory

The fundamental equation relating the tissue concentration as a function of time, $C_t(t)$, the arterial concentration as a function of time (AIF), $C_a(t)$, the perfusion f, and the residue impulse response function, RIF(t), is[13]:

$$C_t(t) = C_a(t) \otimes f\,RIF(t) = f\int_0^t C_a(\tau)RIF(t-\tau)d\tau \qquad (1)$$

The RIF(t) is defined as the CA fraction remaining in the tissue, after a brief injected bolus, directly into the tissue (or voxel), as a function of time. The distribution of transit times, i.e., the fraction of the CA, which leaves the tissue at time t, per time unit, after a bolus injection is the frequency function h(t). The RIF(t) is related to the distribution of transit times, i.e., the frequency function by:

$$RIF(t) = 1 - \int_0^t h(t)d\tau \qquad (2)$$

The mean transit time (MTT) is given as:

$$MTT = \int_0^\infty th(t)dt = \int_0^\infty RIF(t)dt \qquad (3)$$

CTH can be defined as the standard deviation (SD) of the frequency function, h(t):

$$CTH = \sqrt{Var[h(t)]} = \sqrt{\int (t-MIT)^2 h(t)dt} \qquad (4)$$

The frequency function, h(t), can be modeled as a simple gamma-variate function with the parametric form as[14]:

$$h(t)=\left[\left(\frac{1-t_0}{t_{max}-t_0}\right)^{\alpha}\exp\left(\alpha\left(1-\frac{t-t_0}{t_{max}-t_0}\right)\right)\right]\Big/A \quad (5)$$

where t_{max} is time to maximum of the function and t_0 is the time delay from $t=0$ to the time the function begins accounting for the minimal transit time (minimal TT) through the tissue, and A is the total area under the function. Thus, h(t) is normalized to unit area and has three free parameters, t_{max}, t_0, and α, where α is related to the shape. For a given set of these parameters, numerical integration of h(t) according to Eq. [2], gives the residue impulse response function, RIF(t), which subsequently is fitted by use of Eq. [1] to the observed data, also estimating the perfusion f. Therefore, we have four free parameters to fit. Furthermore, for a gamma distribution:

$$MTT=\frac{\alpha+1}{\alpha}t_{max} \quad (6)$$

$$CTH=\frac{\sqrt{\alpha+1}}{\alpha}t_{max} \quad (7)$$

If the BBB is leaky and if permeating CA is irreversibly trapped behind the BBB, at least for the duration of the measurement, corresponding to a subtle increase of the BBB permeability, then Eq. [2] is modulated by a factor of (1-E), where E is the extraction fraction:

$$RIF(t)=1-(1-E)\int_0^t h(\tau)d\tau \quad (8)$$

This means that a fraction, E, of the CA will not leave the brain tissue for the duration of the measurement, and RIF(t) will approach E for longer time values, as h(t) approach unity.

The normal BBB is characterized by very low permeability for a conventional MR CA, and the permeability is often considered to be zero. In diseases with a subtle increase of the BBB permeability, such as multiple sclerosis, small vessel disease, and low-grade brain tumors, the permeability is not very high, meaning that transport from blood to tissue can be considered unidirectional during the observation time and Eq. [8] will be valid. Equation [8] is fully compatible with the formula presented by Schabel,[15] with the modification of assuming an infinitely large extravascular space, which is equivalent with no back diffusion. Thus Eq. [8] is highly suitable in situations with a subtle increase of the BBB permeability, because it avoids inclusion of an additional parameter, the extravascular space. Because only very small amounts of CA enter the extravascular space, the obtained data will not contain any information of this parameter whatsoever. Attempts of estimating the size of the extravascular space from such data will only lead to a reduction in accuracy and precision in the remaining parameters.

The unidirectional clearance constant K_i can be estimated from a Patlak plot[16] and E is then estimated from:

$$E=\frac{f}{K_i} \quad (9)$$

Therefore, K_i enters the model as a free parameter to account for a leaky BBB. However, due to the relatively high number of fitted parameters, f and K_i are estimated separately by use of Tikhonov's generalized singular value decomposition (GSVD) and Patlak's method, respectively, as previously described.[2] These values are then used as initial parameters in the gamma-variate model with five free parameters, avoiding a local minimum in the fitting routine. Schabel[15] has shown that modeling the capillary transit time distribution with a gamma-variate distribution is a generalization of previous suggested models, such as the Tofts model and extended Tofts model,[17] the two-compartment exchange model[18] and the distributed capillary adiabatic tissue homogeneity model.[19] Particularly, Schabel showed that the ratio CTH^2/MTT^2 ($=1/(\alpha+1)$) is bound between zero and one, and characterize the distribution of capillary transit times. The limit $CTH^2/MTT^2 \rightarrow 0$ denotes a delta function capillary transit time distribution compatible with the adiabatic tissue homogeneity model, and the limit $CTH^2/MTT^2 \rightarrow 1$ denotes an exponential capillary transit time distribution compatible with the two-compartment exchange model.

Subjects

HEALTHY SUBJECTS. Twenty-three healthy subjects with a mean age of 32 years (range, 21–52 years, 9 women) were investigated.

PATIENTS. Four clinical patients were studied. The first, a 71-year-old man with a left internal carotid artery (ICA) stenosis and left-sided stroke, with multiple cardiovascular risk factors and previous femoral by-pass surgery. Another 75-year-old female with a left ICA stenosis was included as well as a 70-year-old male with a 3-month-old stroke. Clinical symptoms are described in Table 2. Finally a 37-year-old male was included, who had a reoccurrence of a previously resected glioblastoma, with enhancing lesion component as detected on conventional MRI. He was currently undergoing a radiation treatment regimen.

Ethics

The study was approved by the Ethics Committee of Copenhagen County according to the standards of The National Committee on Health Research Ethics, protocol number H-D-2008-002. All experiments were conducted in accordance with the Declaration of Helsinki 1975 and all subjects gave written informed consent.

DCE-MRI

The DCE MRI experiments were performed using a 3.0 Tesla (T) Philips Achieva (Philips Medical Systems, Best, The Netherlands) and a 32-element phased-array receive head coil. A two-dimensional (2D) saturation recovery gradient recalled sequence was used both for an initial T_1 measurement and for the subsequent dynamic imaging. Each slice was acquired after application of a nonselective saturation prepulse with a saturation time delay (*TD*). Echoes were read with an radiofrequency flip angle of 30°, repetition time of 3.82 ms, echo time of 1.9 ms, centric phase ordering, scan matrix size 96×61 (interpolated to 256×256), SENSE factor 2, field of view (FOV) $240\times182\,mm^2$ and 5 slices of 8 mm thickness resulting in an acquired spatial resolution of $2.5\times3.1\times8\,mm^3$. The T_1 measurement was performed by varying the *TD* value (120 ms, 300 ms, 600 ms, 1 s, 2 s, 4 s, 10 s).

The passage of the bolus of the CA was imaged using a fixed *TD* of 120 ms. The most caudal slice was (independently of the other slices) placed orthogonally to the ICA based on an MR

TABLE 1. Values Based on the Gamma-Variate Model From 23 Healthy Subjects

Percentile 2.5% 25% 50% 75% 97.5%	R_1 (1/s)	CBF (mL/100g/min)	CBV (mL/100g)	MTT (s)	CTH (s)	CTH^2/MTT^2	K_i (mL/100g/min)
Frontal WM n=23							
	0.86	6.0	0.8	3.3	0.09	0.000	0.006
	0.99	9.2	1.1	4.3	0.67	0.011	0.025
	1.02	**12.1**	**1.8**	**5.2**	**2.44**	**0.130**	0.094
	1.07	14.8	1.9	6.3	3.78	0.365	0.112
	1.29	22..7	2.9	8.2	6.41	0.763	0.140
Thalamus n=23							
	0.67	10.6	0.6	2.6	0.01	0.000	0.001
	0.71	15.7	1.5	3.7	0.15	0.001	0.033
	0.75	**19.8**	**1.7**	**4.1**	**0.35**	**0.006**	0.064
	0.77	23.9	1.9	4.7	1.69	0.073	0.091
	0.93	29.8	2.2	6.6	3.75	0.335	0.183
Putamen n=23							
	0.64	14.7	1.2	1.7	0.00	0.000	0.011
	0.68	26.6	1.6	2.3	0.40	0.008	0.029
	0.69	**31.5**	**1.8**	**3.0**	**0.93**	**0.062**	**0.070**
	0.72	41.8	2.1	3.3	1.73	0.232	0.118
	0.86	51.9	3.0	3.8	2.91	0.659	0.286

angiogram to obtain an arterial input function (AIF) with minimal partial volume. In total 350 frames, with a time resolution of 1.25 s, were obtained. Both modulus, real and imaginary images were stored. The dose of CA Gadovist® (1.0 mmol/mL) was 2×0.045 mmol/kg (in the patient with brain tumor only one injection was given: 1×0.045 mmol/kg), and the CA was injected with 3 mL/s followed by 20 mL saline using an automatic CA injector (Medrad Spectris Solaris MR injector system) at time 15 and again after 70 frames (only after 15 in the patient with brain tumor). The magnitude of the dose was based on a compromise between increasing the CNR for a higher dose and the possibility of introducing a T_2^* effect or truncation of the bolus peak of the AIF. Anatomical turbo spin echo images with high spatial resolution (acquired matrix size of 512×512, FOV 240 mm, 8 mm slice thickness, acquisition time 2 min) were obtained corresponding to the five perfusion slices.

The relationship between the MR signal and CA concentration is not linear, but the change of R_1 (ΔR_1) is proportional to the CA concentration with regard to both blood and tissue. When using centric phase ordering, the MR signal, $s(t)$, as a function of time t, $\Delta R_1(t)$ and concentration $C(t)$ are related by:

$$s(t)=M_0\sin(\alpha)[1-\exp\left(-TD\left(R_1+\Delta R_1(t)\right)\right)], \Delta R_1(t)=r_1 C(t) \quad (10)$$

The relaxivity r_1 of Gd-DTPA at 3T was set to 4 s^{-1} mM^{-1}, a textbook value provided by the Bayer Pharma AG, producer of Gadovist®. Equal relaxivities were assumed for the intravascular compartment and for the tissue in general. The signal equation for a saturation recovery (Eq. [10] with $\Delta R_1 = 0$) was fitted to the data obtained for varying TD to determine T_1 and M_0. The MR signal was converted to ΔR_1 during the bolus passage as a single point resolved T_1 determination, assuming a fast water exchange regime.[20] The pixels in the center of the ICA were used for the input function. This arterial input function was further scaled with a venous outflow curve obtained from the sagittal sinus to reduce the partial volume effect. A possible partial volume effect of the venous outflow curve was effectively eliminated using the modulus and phase information.[21,22]

CTH Estimation

Calculations were performed both for selected regions of interest (ROIs) and pixelwise with the purpose of creating parameter maps. In the 23 healthy subjects, one ROI was placed in the thalamus, one in the putamen and one in the frontal white matter. In both patients with internal carotid stenosis, ROIs was placed in the hypo-perfusion area of the left frontal gray/white matter and a symmetric contralateral area in normal perfused gray/white matter as well as the basal ganglia in both hemispheres. In the patient with a 3-month-old stroke were placed ROIs in the stroke region and in the contralateral apparently healthy brain tissue as well as the basal ganglia. Finally, in the

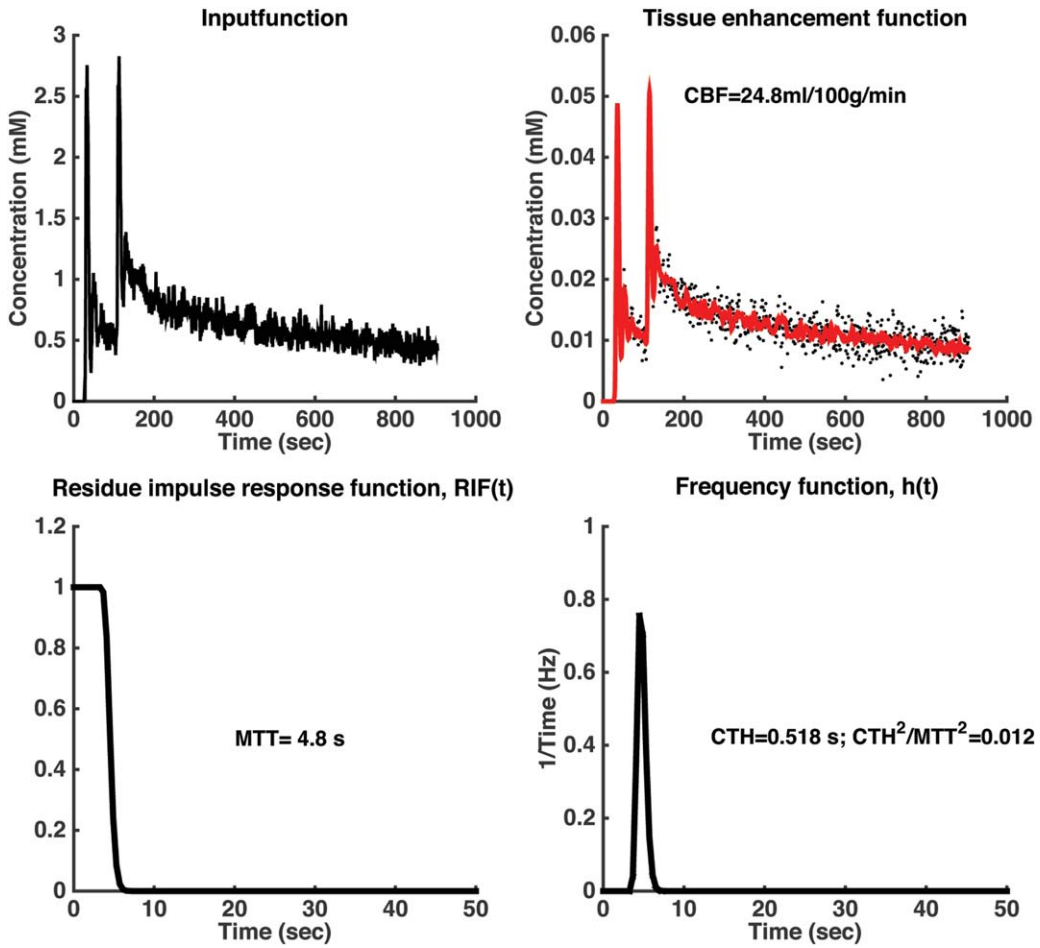

FIGURE 1: An example of calculation from an ROI placed in the thalamus of a young healthy subject. Note the symmetrical shape of the h(t) function and that RIF(t) stays at a value of 1 for approximately 3 s, which correspond to the minimal TT for that ROI. The MTT, i.e., the area under the RIF(t) is 4.8 s. MTT, CTH, and CTH^2/MTT^2 values are inserted.

patient with brain tumor, an ROI was placed in the enhancing part of the tumor. ROIs were placed carefully avoiding partial volume effects, especially from larger vessels. The size of the individual ROIs in white matter was approximately 1 cm^2. The ROIs were drawn on the corresponding high-resolution anatomical image.

The obtained dynamic data were interpolated to a higher time resolution with a factor of 3 before any calculation to reduce discretization inaccuracy in the calculations. After conversion of MR signal to concentration of CA, the gamma-variate model imbedded in Eq. [1] and Eq. [2] was fitted to data. So far, we have assumed that there is no delay in the CA arrival between the AIF and the tissue curve, here called the bolus arrival delay time. This is not always true and one has to shift either of the curves to synchronize bolus arrival in tissue with the AIF. This was accomplished by fitting a short segment of a gamma-variate function to the AIF and the tissue curve starting with the baseline points and ending a few points after peak enhancement. This fit directly gives an estimate of the starting point of the enhancement of blood and tissue, see Eq. [5]. This allowed us to shift the AIF so that the bolus arrival time corresponded to that of the initial tissue enhancement. This was done before fitting the tracer kinetic model to data from ROIs or pixel wise calculations. The variance of the estimated h(t) was calculated using Eq. [4]. In addition, the ratio CTH^2/MTT^2 was also calculated.

Results

Healthy Controls

In the 23 healthy controls, we find symmetric h(t) functions with an average CTH of 0.93 s (interquartile range [IQR] 1.33 s) and CTH^2/MTT^2 of 0.062 (IQR 0.22) in putamen gray matter, compatible with a homogenous delivery of nutrients through the capillary bed (see Table 1). Spearman nonparametric correlation analysis showed an inverse correlation between capillary heterogeneity and blood flow estimated with Tikhonov GSVD (thus entirely independent from the CTH estimation) in putamen gray matter ($cc = -0.472$; $P = 0.023$) and in frontal white matter ($cc = -0.438$; $P = 0.037$). This inverse relationship where high blood flow is equal to a more homogenous capillary delivery is also reflected in white matter, where CBF is significantly lower ($t = 8.9$; $P = 0.1 \times 10^{-11}$) and CTH values significantly higher ($t = -3.6$; $P = 0.001$) when compared with their respective values in putamen gray matter.

A Mann Whitney U-test showed higher blood flow (for both the Tikhonov and the adiabatic tissue model) in females compared with males in putamen ($P = 0.027$) and white

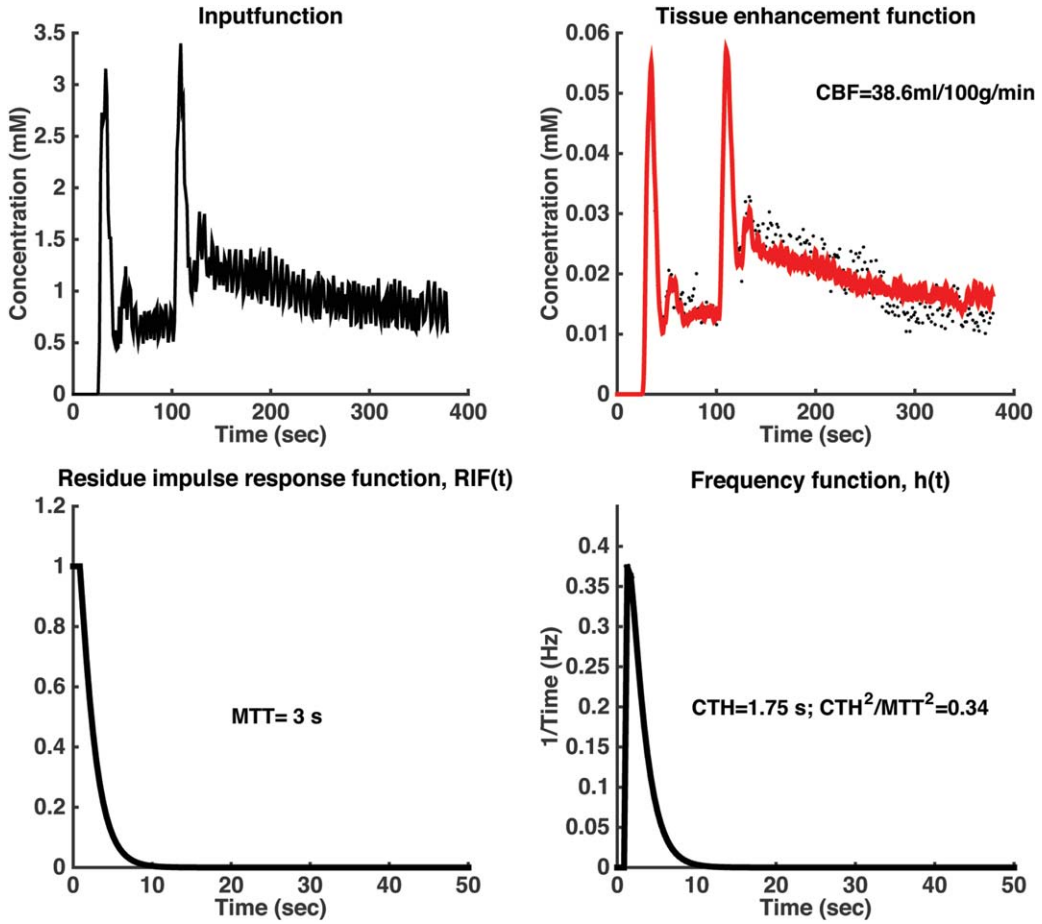

FIGURE 2: An example of calculation from an ROI placed in frontal gray/white matter of a 71-year-old man having internal carotid stenosis contralateral to the ROI placement.

matter ($P = 0.025$), but apart from this we observed no gender or age effects on the estimated PK values (Mann Whitney U-test and Spearman correlation analysis). We found no time delay of bolus arrival between the tissue curve and the AIF in the healthy subjects. The method allows estimation of R_1, CBF, CBV, MTT, and Ki in addition to CTH and CTH^2/MTT^2. A typical example of an ROI placed in the thalamus of a healthy control can be seen in Figure 1, and pixelwise maps from the same subject in Figure 5.

PATIENTS. In the 71-year-old male stroke patient with a complete occlusion of the left sided ICA, we observe a marked difference between h(t) functions between the contralateral and ipsilateral hemispheres (Figs. 2 and 3). In the contralateral "unaffected" hemisphere we observe a slightly asymmetrical h(t) function with a CTH of 1.8 s and a CTH^2/MTT^2 of 0.34. In the ipsilateral, possibly ischemic left frontal gray/white matter of the same patient with the left internal carotid stenosis, the h(t) function is highly asymmetric with a CTH of 4.3 and a CTH^2/MTT^2 of 0.21. Pixelwise maps of one selected slice of this patient is shown in Figure 6. A similar hemisphere difference is observed in the 75-year-old female with similar clinical picture (Table 2). Thus in these two patients we observe an absolute hemisphere difference of 33–238% and much higher than values from the healthy controls. However, CTH^2/MTT^2 is high in both hemispheres, signifying a more exponential like distribution of capillary transit times. In a 70-year-old male with a 3-month-old stroke and no carotid artery occlusion, we find no differences between the hemispheres or in the stroke region.

The investigated patient with a brain tumor showed leakage of the BBB in the tumor itself, which is evident when observing the tissue enhancement curve (Fig. 4), i.e., the slope of the tail is markedly increased compared with nonenhancing tissue curves (Figs. 1–3). The h(t) shows asymmetry, and RIF(t) approaches a constant level at a value of around 0.18, which reflects the estimated extraction fraction. If this additional parameter is eliminated from the fit, then the fit becomes extremely poor. CTH is high and CTH^2/MTT^2 is much higher than seen in healthy tissue. Pixelwise maps of one selected slice of the tumour patient is shown in Figure 7.

To compare performance of perfusion estimation by the gamma-variate model and the Tikhonov's GSVD, we conducted correlation analysis and found a correlation coefficient of 0.97 ($P < 0.001$). A Bland-Altman plot showed a bias of 1.9 (SD 3.9) mL/100 g/min in favor of the gamma-variate model.

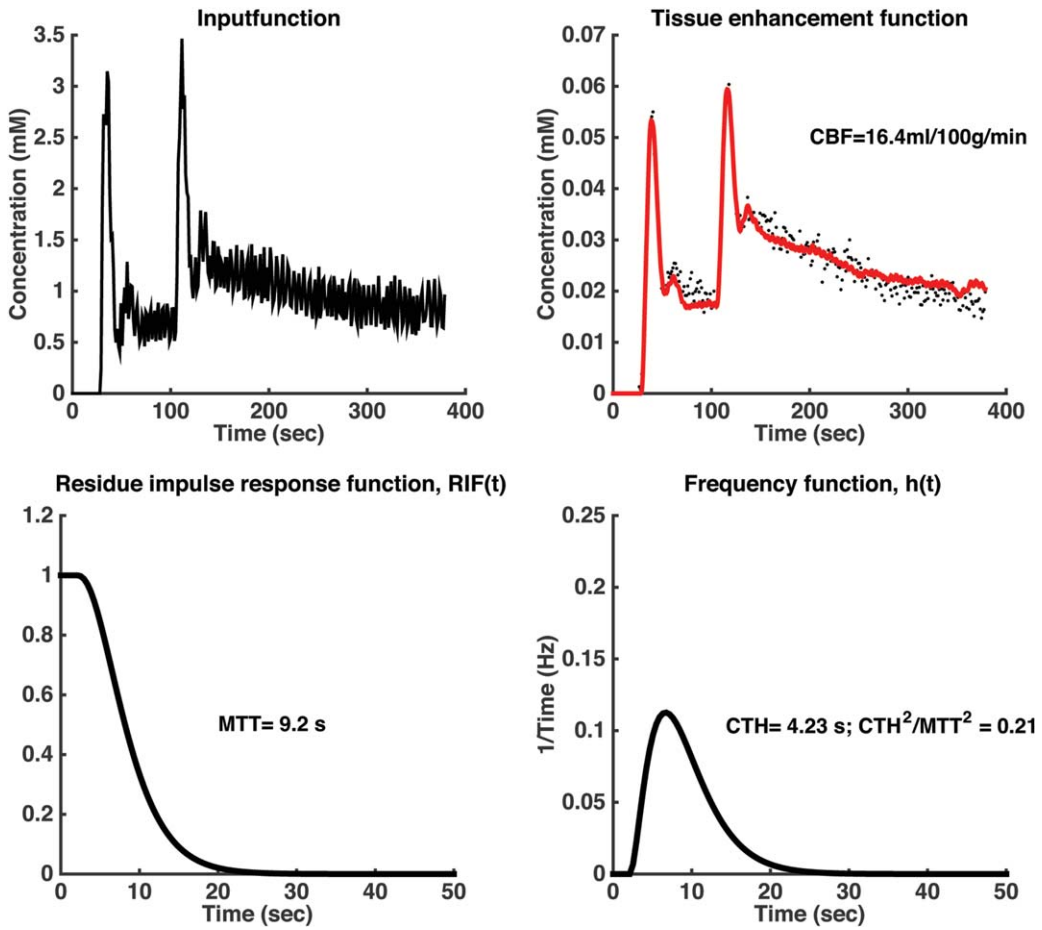

FIGURE 3: An example of calculation from an ROI placed in frontal gray/white matter ipsilateral to an internal carotid stenosis in a 71-year-old man (same subject as in Fig. 2). MTT, CTH, and CTH^2/MTT^2 values are inserted. Note the asymmetry of h(t) signifying a large heterogeneity in capillary transit times.

Discussion

In this study, we have developed a relatively simple method that allows us to estimate the distribution of in vivo capillary transit times in the healthy human brain, using dynamic contrast-enhanced T_1-weighted MRI (DCE-MRI). The approach follows the basic idea of Schabel,[15] who modeled the capillary transit time as a gamma-variate distribution. Our main finding is the capillary transit time heterogeneity is quite small with a delta-function like h(t) distribution in normal subjects. In addition, our values of CTH in healthy controls are quite distinct from CTH values in the two patients with complete internal artery occlusion and the patient with a brain tumor investigated in this study, and these results are in line with values reported by Schabel[15] from three patients with brain tumors.

The so-called frequency function h(t), modeled as a gamma-variate function, represents the distribution of transit times, and we have shown that it is a narrow symmetrical function with CTH values around 0.6 s in healthy gray matter of young subjects and higher in white matter, presumably related an inverse correlation between perfusion and capillary heterogeneity. CTH values have previously been measured in brain capillaries of rats, using confocal laser-scanning microscopy or intravital video microscopy, with typical values of CTH in resting condition between 1 and 1.3 s, while activation (electrical stimulation, hypoxemia, hypercapnia) decreased CTH to around 0.2–0.7.[23–25] Thus, our CTH values in healthy human brain tissue are comparable to those found in rat brains during various types of stimulation. A likely explanation for the difference could be some degree of arousal of the humans lying inside the noisy scanner, while the rats are anesthetized. In brain tissue, supplied by a stenotic artery, potentially suffering from lack of oxygen, the h(t) shows a pronounced asymmetry with a much larger variance. The CTH values we find in healthy subjects show a homogenous distribution, while both patients with complete carotid stenosis and the patient with a brain tumor investigated in this study have CTH values that differ substantially from the healthy controls. This is in line with previous study of three brain tumor patients by Schabel.[15]

The h(t) configuration has previously been theorized to provide important information of the capillary blood to tissue transport capability. Jespersen and Østergaard have

TABLE 2. Clinical Information and PK Values From the Four Patients Included in the Study

			Right hemisphere			Left hemisphere		
Subject	**Age/gender**	**ROI location**	**CBF (mL/100g/min)**	**MTT (s)**	**CTH (s)**	**CBF (mL/100g/ min)**	**MTT (s)**	**CTH (s)**
1	75-year-old female	Putamen gray matter	44.7	2.4	2.1	21.6	6.5	2.8
2	71-year-old male	Putamen gray matter	36.4	3.46	0.92	35.6	4.0	2.0
3	70-year-old male	Infarct in left hemisphere and contralateral WM[a]	14.3	4.3	1.1	9.3	5.5	1.0
4	34-year-old male	GBM in left hemisphere and contralateral WM	21.8	2.7	2.0	10.7	9.0	8.7

Clinical info	
Subject 1	Complete left ICA occlusion, coronary bypass, previous ischemic symptoms from left hemisphere, cognitive impairment, at time of scan acute TIA with aphasia and balancing problems
Subject 2	Complete left ICA occlusion, multiple cardiovascular risk factors, old lacunar infarcts, at time of scan acute TIA with aphasia, right sided central facial nerve palsy, right upper extremity palsy.
Subject 3	Three months old infarct in left capsula interna crus postrema, with right upper extremity palsy and aphasia
Subject 4	Glioblastoma in the left parietoteporal region. Previously resected, by now reoccurred

[a]No hemisphere differences were observed in the basal ganglia of this subject.

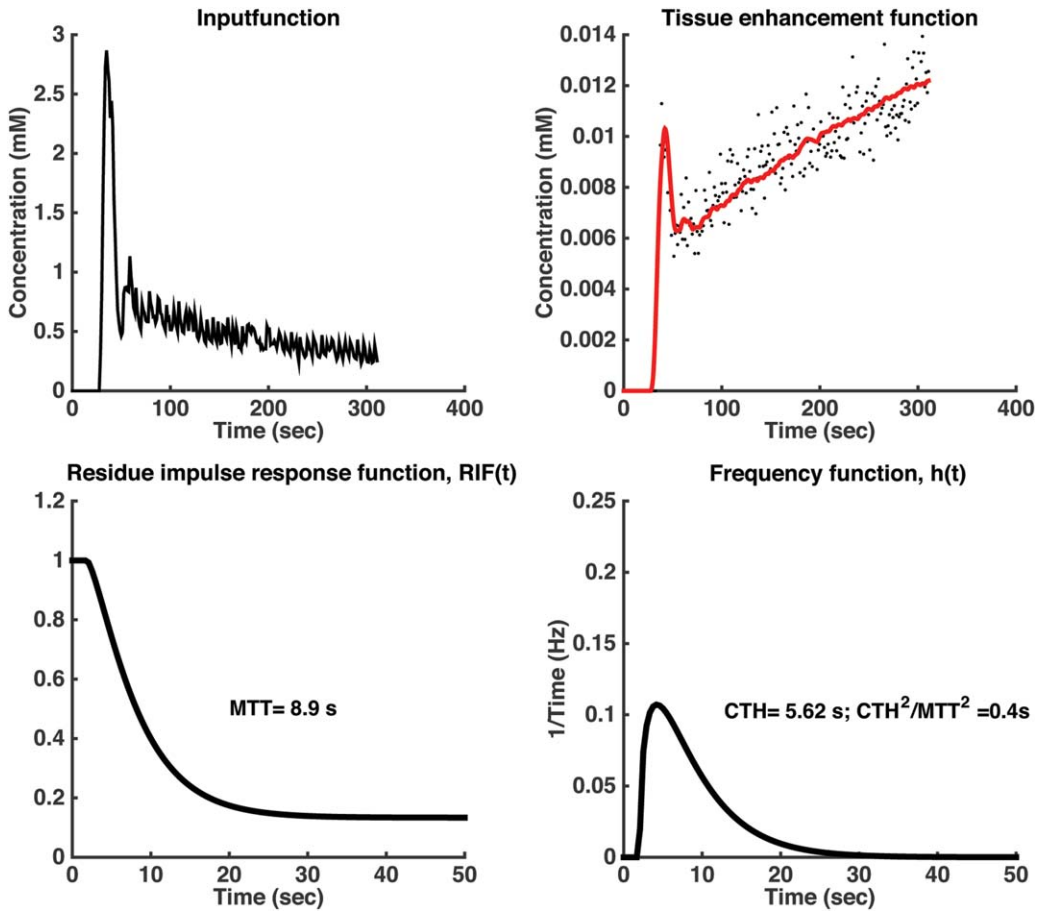

FIGURE 4: An example of calculation from an ROI placed in a tumor with leaky BBB. Note the asymmetry of h(t), and also that the RIF reaches a plateau at around 0.18 corresponding to the extraction fraction of the CA. CTH^2/MTT^2 is higher compared with normal tissue. Note that MTT refer to capillary transit times and excludes CA having passed the BBB. Thus, MTT is accordingly smaller than the area under the residue impulse response function.

shown that the h(t) distribution may set the limit for the maximum oxygen extraction fraction encountered in brain tissue.[5] Evidently, this also dependents on the exact BBB permeability of oxygen, but the h(t) distribution may very well have impact on other substances being transported from the blood to the brain tissue, including toxic substances.

Modeling the distribution of transit times in case of a leaky BBB constitute a special challenge. The model represented by Eq. [5] is well suited for an intra-vascular CA with no or minimal leakage over the BBB. Conventional brain MRI CA is normally considered strictly intravascular. It has previously been demonstrated that subtle leakage can be measured in healthy subjects, and a higher but still small leakage can be measured in periventricular normal appearing white matter in patients with multiple sclerosis and patients with optic neuritis.[10,26] In patients with brain tumors, leakage is often seen, and it is well known that the BBB permeability can range from zero to very high levels of permeability similar to what is encountered in capillaries outside the brain, although this is rare.

However, it is possible to incorporate some degree of leakage into the model. The area of the h(t) is normalized to one, meaning that the entire amount of CA leaves the tissue. If a small fraction of CA is bound "irreversible" in the tissue, i.e., no back diffusion from tissue to blood occurs during the measurement period, then the area of h(t) is reduced to (1-E) times h(t), where E is the extraction fraction. This step is important when estimating the residue impulse response function. Introducing this modification corresponding to Eq. [8], improved the fit remarkably, see Figure 4. However, in cases with higher permeability, the model represented by Eq. [8] is not adequate and the full model developed by Schabel[15] should be used, where the interstitial volume is added as an additional free parameter to be estimated. This additional parameter should only be included if the measured tissue data contain such information, i.e., if back diffusion occurs during the measuring period. Otherwise, data may be over-fitted and parameter precision and accuracy become poor.

A pertinent question is whether the frequency function, h(t), which literally represents the outflow of the CA from the tissue volume, can be described analytically as a gamma-variate function. Schabel[15] have shown that the gamma-variate model is a more general model encompassing both the common two-compartment exchange model[2,18] and the adiabatic tissue homogeneity model[19] as two opposite extremes of the gamma-variate

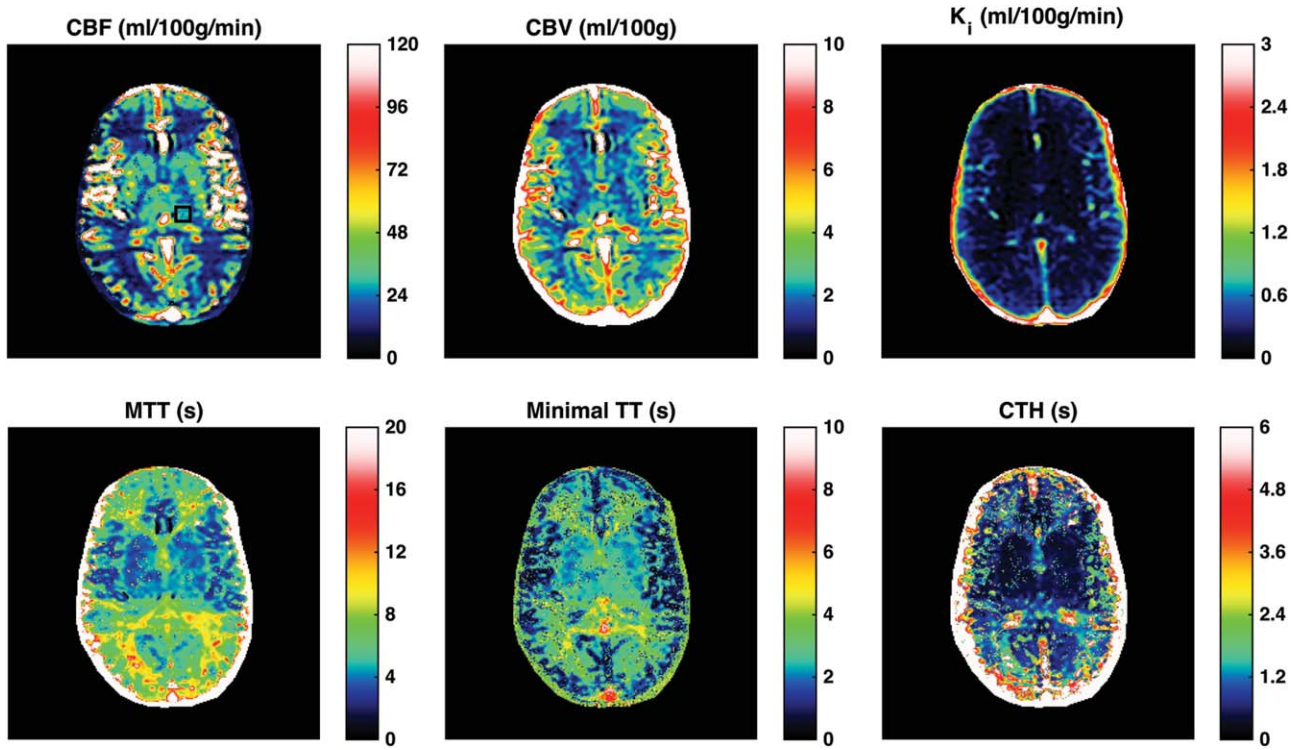

FIGURE 5: Pixel wise calculated maps of CBF, CBV, permeability K_i, MTT, minimal TT, and CTH, from a healthy subject. The results from the ROI on the CBF map are shown in Figure 1.

model, with a corresponding distribution of capillary transit times as an exponential distribution ($CTH^2/MTT^2 \rightarrow 1$) and a delta function ($CTH^2/MTT^2 \rightarrow 0$), respectively. Due to a low voxel SNR of 7 in the DCE data, Schabel was only able to analyze voxels within brain tumor regions with high degree of enhancement where he found values (CTH^2/MTT^2) around 0.2–1.

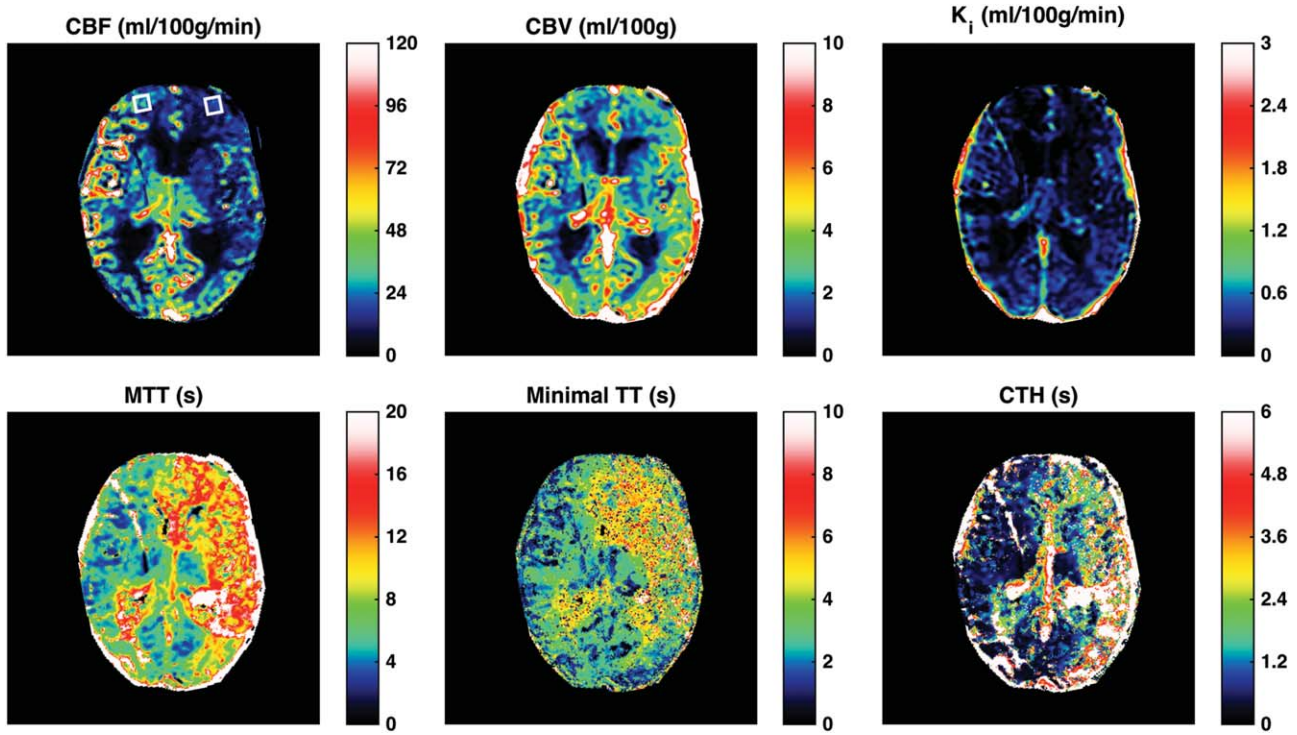

FIGURE 6: The figure shows results from a 71-year-old man with a complete left sided internal carotid stenosis and multiple thrombo-embolic episodes. Perfusion (CBF) is decreased while the CBV is increased in the fronto-parietal region, but the permeability (K_i) seems relatively normal. The MTT, the minimal TT, and CTH are prolonged in the entire region showing altered perfusion.

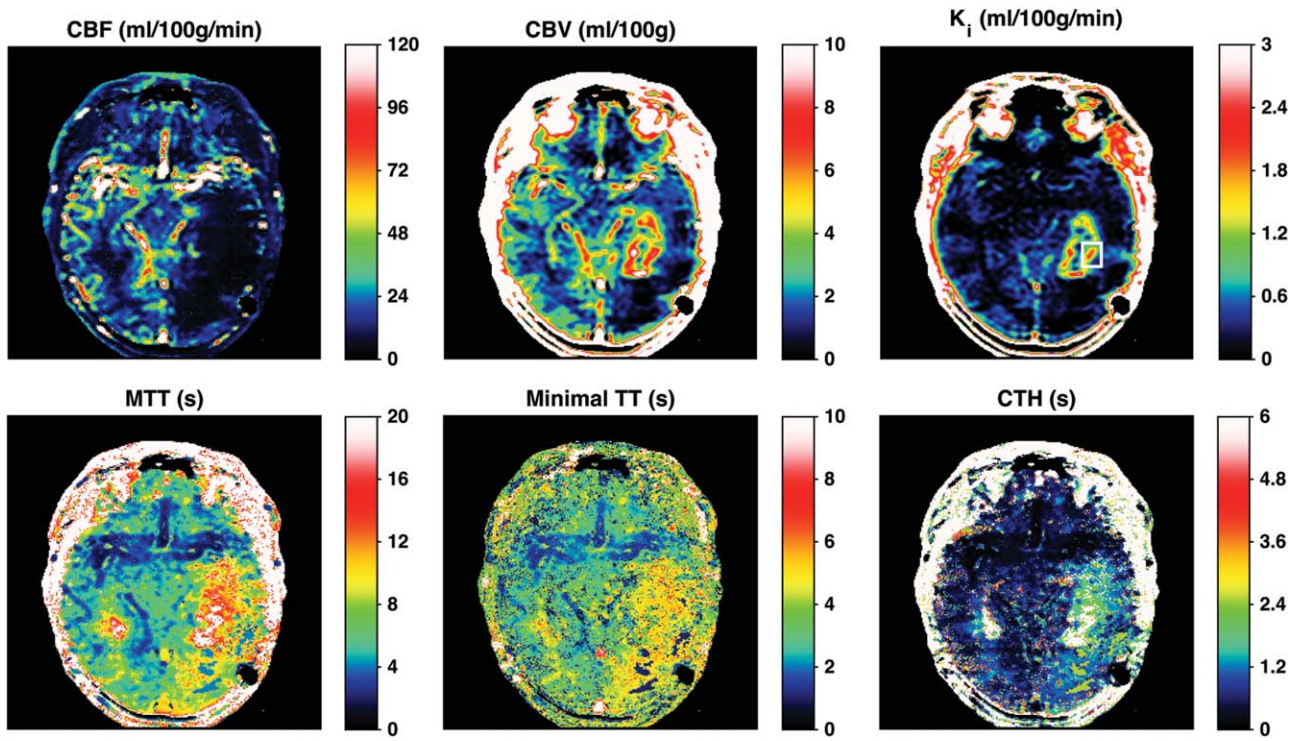

FIGURE 7: The results of a patient with reoccurrence of a glioblastoma, showing diminished perfusion (CBF) in the parieto-temporal region, and a central part showing leakiness (K_i) up to 2 mL/100 g/min. The MTT is prolonged in the region showing leakiness, but also outside in a larger region nearly corresponding to the area showing decreased perfusion. The CTH is large in the tissue showing leakiness, but even larger in the core with diminished leakiness.

Furthermore, he found that the two-compartment exchange model and the gamma-variate distribution model performed equally well. In the three clinical examples where we found altered CTH values, we did also notice values of CTH^2/MTT^2 around 0.2–0.4 in the affected brain tissue. However, in the healthy subjects, we found CTH^2/MTT^2 one order of magnitude lower, around 0.02–0.1, signifying that perfusion and transit time distribution is quite homogeneous, resembling a delta-function. Thus, the adiabatic tissue homogeneity model seems more appropriate as a model for perfusion in healthy human brain tissue.

From the present study, it cannot be shown whether CTH provides additional information compared with MTT. Obviously, these measures are correlated, as seen from our data. However, a necessary requirement is an accurate and reproducible estimation of the CTH value either based on ROI or pixel wise calculation. In the study of Schabel the SNR was approximately 6, using a scanner field strength of 1.5T, and the uncertainty of CTH was very large.[15] Our study was performed at a higher field strength of 3T with a SNR of approximately 70 and a CNR of approximately 7 for single voxel in white matter.[1] The precision of our CTH values is acceptable on an ROI basis; however, when calculated pixel wise, the CTH images become noisier, and improvement is desirable. Schabel pointed to the importance of obtaining data with a sufficient time resolution, heuristically set to 3 $\Delta t < MTT$, where Δt is the time between data points acquired. Our time resolution of 1.25 s is compatible with this requirement, but even higher time resolution may be beneficial for accurate estimation of h(t) and RIF(t).

Also, the bolus arrival time in tissue may be of importance. If the AIF and tissue enhancement curve is wrongly synchronized, this may transform to an altered configuration of h(t) and RIF(t) and, therefore, CTH. It may also be important to reduce the number of free parameters that have to be estimated, especially in the presence of a leaky BBB. Perfusion f and the permeability constant K_i can be estimated separately by use of Tikhonov's GSVD and Patlak's method, respectively, reducing the number of free parameters to be estimated in the gamma-variate model. It is interesting to note that the perfusion estimated from Tikhonov's method and the perfusion estimated from the gamma-variate model in the healthy subjects (no BBB defect) yields very similar results, even though the configurations of RIF(t) from the two methods are quite different. The imbedded regularization in Tikhonov's method does not favor the initial plateau and a nonzero minimal transit time as the gamma-variate method does.

We have previously been able to estimate CBF successfully from DCE-MRI data based on Tikhonov GSVD,[1] and there is good agreement between this approach and the estimates presented in this study using the gamma-variate distribution model. The absolute perfusion values are slightly lower than typical PET values from the literature, where gray matter perfusion is

typically in the range of 40–60 mL/100 g/min.[27,28] However, we find a gray matter/white matter perfusion ratio of 3, which is supported by several other studies.[28,29] Our values of blood volume are in the range of 2–5 mL/100g/min reported in post-mortem studies[30] and from PET studies.[28,29] Our MTT values are in the typical range of 3–5 s, reported by PET[28] and MRI perfusion studies.[31,32]

Study Limitations

Because this is a small exploratory study, there are some inherent limitations, the most important being small cohort size, only four subjects with pathological changes studied and finally no external validation.

In conclusion, we have shown that it is possible to calculate the distribution of capillary transit times from DCE-MRI at 3T, giving a measure of capillary transit time heterogeneity. The clinical impact of this measure awaits further studies of both healthy subjects and various brain pathologies to establish reference values in health and disease as well as determining the relationship with other physiological brain metrics, such as CBF, CBV, MTT, and cerebral metabolic rate of oxygen.

References

1. Larsson HBW, Hansen AE, Berg HK, Rostrup E, Haraldseth O. Dynamic contrast-enhanced quantitative perfusion measurement of the brain using T1-weighted MRI at 3T. J Magn Reson Imaging 2008; 27:754–762.
2. Larsson HBW, Courivaud F, Rostrup E, Hansen A. Measurement of brain perfusion, blood volume, and blood-brain barrier permeability, using dynamic contrast-enhanced T1-weighted MRI at 3 tesla. Magn Reson Med 2009;62:1270–1281.
3. Sourbron S, Ingrisch M, Siefert A, Reiser M, Herrmann K. Quantification of cerebral blood flow, cerebral blood volume, and blood-brain-barrier leakage with DCE-MRI. Magn Reson Med 2009;62:205–217.
4. Kuschinsky W, Paulson OB. Capillary circulation in the brain. Cerebrovasc Brain Metab Rev 1992;4:261–286.
5. Jespersen SN, Østergaard L. The role of cerebral blood flow, capillary transit time heterogeneity, and oxygen tension in brain oxygenation and metabolism. J Cereb Blood Flow Metab 2012;32:264–277.
6. Stefanovic B, Hutchinson E, Yakovleva V, et al. Functional reactivity of cerebral capillaries. J Cereb Blood Flow Metab 2008;28:961–972.
7. Crone C. The permeability of capillaries in various organs determined by use of the indicator diffusion method. Acta Physiol Scand 1963;58: 292–305.
8. Renkin EM. Transport of potassium-42 from blood to tissue in isolated mammalian skeletal muscles. Am J Physiol 1959;197:1205–1210.
9. Masamoto K, Kershaw J, Ureshi M, et al. Apparent diffusion time of oxygen from blood to tissue in rat cerebral cortex: implication for tissue oxygen dynamics during brain functions. J Appl Physiol 2007;103: 1352–1358.
10. Cramer SP, Modvig S, Simonsen HJ, Frederiksen JL, Larsson HBW. Permeability of the blood-brain barrier predicts conversion from optic neuritis to multiple sclerosis. Brain 2015;138:2571–2583.
11. Starr JM, Farrall AJ, Armitage P, McGurn B, Wardlaw J. Blood-brain barrier permeability in Alzheimer's disease: a case-control MRI study. Psychiatry Res 2009;171:232–241.
12. Taheri S, Gasparovic C, Huisa BN, Adair JC, Edmonds E, Prestopnik J. Blood-brain barrier permeability abnormalities in vascular cognitive impairment. Stroke 2011;42:2158–2163.
13. Meier P, Zierler KL. On the theory of the indicator-dilution method for measurement of blood flow and volume. J Appl Physiol 1954;6: 731–744.
14. Madsen MT. A simplified formulation of the gamma variate function. Phys Med Biol 1992;37:1597–1600.
15. Schabel MC. A unified impulse response model for DCE-MRI. Magn Reson Med 2012;68:1632–1646.
16. Patlak CS, Blasberg RG. Graphical evaluation of the blood-to-brain transfer constants from multiple-time uptake data. Generalizations. J Cereb Blood Flow Metabol 1985;5:584–590.
17. Tofts PS, Brix G, Buckley DL, et al. Estimating kinetic parameters from dynamic contrast-enhanced T1-weighted MRI of a diffusible tracer: standardized quantities and symbols. J Magn Reson Imaging 1999;10: 223–232.
18. Brix G, Semmler W, Port R, Schard LR, Layer G, Lorenz WJ. Pharmacokinetic parameters in CNS Gd-DTPA enhanced MR imaging. J Comput Assist Tomogr 1991;15:621–628.
19. St. Lawrence KS, Lee TY. An adiabatic approximation to the tissue homogeneity model for water exchange in the brain: I. Theoretical derivation. J Cereb Blood Flow Metab 1998;18:1365–1377.
20. Larsson HBW, Rosenbaum S, Fritz-Hansen T. Quantification of the effect of water exchange in dynamic contrast MRI perfusion measurements in the brain and heart. Magn Reson Med 2001;46:272–281.
21. Hansen A, Pedersen H, Rostrup E, Larsson HBW. Partial volume effect (PVE) on the arterial input function (AIF) in T_1-weighted perfusion imaging and limitations of the multiplicative rescaling approarch. Magn Reson Med 2009;62:1055–1059.
22. Van Osch MJP, Vonken EPA, Bakker CJG, Viergever MA. Correcting partial volume artifacts of the arterial input function in quantitative cerebral perfusion MRI. Magn Reson Med 2001;45:477–485.
23. Villringer A, Them A, Lindauer U, Einhäupl K, Dirnagl U. Capillary perfusion of rat brain cortex. An in vivo confocal microscopy study. Circ Res 1994;75:55–62.
24. Hudetz AG, Biswal BB, Feher G, Kampine JP. Effects of hypoxia and hypercapnia on capillary flow velocity in the rat cerebral cortex. Microvasc Res 1997;54:35–42.
25. Schulte ML, Wood JD, Hudetz AG. Cortical electric stimulation alters erythrocyte perfusion pattern in the cerebral capillary network of the rat. Brain Res 2003;963:81–92.
26. Cramer SP, Simonsen H, Frederiksen JL, Rostrup E, Larsson HBW. Abnormal blood-brain barrier permeability in normal appearing white matter in multiple sclerosis investigated by MRI. Neuroimage Clin 2013;4:182–189.
27. Iida A, Okazawa H, Hayashida K, et al. Database of normal human cerebral blood flow, cerebral blood volume, cerebral oxygen extraction fraction and cerebral metabolic rate of oxygen measured by positron emission tomography with 15 O-labelled carbon dioxide or water, carbon monoxide and oxygen. Eur J Nucl Med Mol Imaging 2004;31:635–643.
28. Rostrup E, Knudsen GM, Law I, Holm S, Larsson HBW, Paulson OB. The relationship between cerebral blood flow and volume in humans. Neuroimage 2005;24:1–11.
29. Law I, Iida H, Holm S, et al. Quantitation of regional cerebral blood flow corrected for partial volume effect using O-15 water and PET: II. Normal values and gray matter blood flow response to visual activation. J Cereb Blood Flow Metab 2000;20:1252–1263.
30. Bassingthwaighte JB. Microcirculatory considerations in NMR flow imaging. Magn Reson Med 1990;14:172–178.
31. Sourbron S, Ingrisch M, Siefert A, Reiser M, Herrmann K. Quantification of cerebral blood flow, cerebral blood volume, and blood-brain-barrier leakage with DCE-MRI. Magn Reson Med 2009;62:205–217.
32. Helenius J, Perkio J, Soinne L, et al. Cerebral hemodynamics in a healthy population measured by dynamic susceptibility contrast MR imaging. Acta Radiol 2003;44:538–546.